

The influence of the of sheds geometry on the pressure coefficients of the surface of the closed buildings

A influência da geometria de sheds na distribuição de coeficientes de pressão na superfície de edifícios vedados

Marieli Azoia Lukiantchuki^{a*}, Alessandra Prata Shimomura^b,
Fernando Marques da Silva^c, Rosana Maria Caram^d

a Universidade Estadual de Maringá,
Departamento de arquitetura e
urbanismo. Maringá-PR, Brasil.

*E-mail: malukiantchuki2@uem.br

b Universidade de São Paulo,
Faculdade de Arquitetura e
Urbanismo. São Paulo-SP, Brasil.

c Laboratório Nacional de Engenharia
Civil. Lisboa, Portugal.

d Universidade de São Paulo, Instituto
de Arquitetura e Urbanismo. São
Carlos-SP, Brasil.

Palavras-chave:

ventilação natural, coeficiente
de pressão, simulação CFD,
geometria dos edifícios, sheds.

Keywords:

*natural ventilation, pressure
coefficient, CFD simulation,
geometry building, shed roof.*

Resumo

O conhecimento da distribuição de pressão das superfícies dos edifícios é importante para a avaliação de cargas de vento e da ventilação natural. As distribuições de pressão induzidas pelo vento são influenciadas por uma ampla gama de fatores, incluindo as condições do entorno urbano e a geometria do edifício. No entanto, a maioria desses estudos é focada em edifícios de geometrias simples e não em geometrias mais complexas como edifícios com sheds na cobertura. A falta de dados para edifícios com formatos mais complexos faz com que os projetistas usem bancos de dados existentes para edifícios simplificados, o que não é compatível com a distribuição de pressão nas superfícies dos edifícios com geometrias complexas. Neste estudo, investigou-se a influência da geometria dos edifícios na distribuição dos coeficientes de pressão nas superfícies de edifícios vedados. Quatro modelos foram avaliados: o caso de referência com uma geometria simples (paralelepípedo) e três modelos de edifícios com sheds na cobertura: o modelo um apresenta sheds com formato ortogonal e os modelos dois e três, com sheds que apresentam geometrias aerodinâmicas. A metodologia utilizada foram simulações com base em Dinâmica dos Fluidos Computacional (CFD). Os resultados mostram que edifícios com sheds na cobertura proporcionam mudanças significativas na distribuição de pressão na superfície dos edifícios, devido às múltiplas áreas de separação do fluxo de ar e recirculações de ar ao longo das fachadas. Além disso, mudanças significativas foram identificadas nos edifícios com sheds aerodinâmicos em relação aos sheds ortogonais.

Abstract

Knowledge of the pressure distribution on building walls is important for the evaluation of wind loads and natural ventilation. Wind induced pressure distributions are influenced by a wide range of factors including urban surroundings and building geometry. However, the majority of these studies focused on simple building geometries without volume details such as shed roof. The lack of data for complex geometries leads designers to use existing databases for simple geometries which is not compatible with the pressure distribution on the building surfaces with complex geometries. In this study, the influence of geometry building on pressure coefficient distribution around closed buildings was investigated. Four models were evaluated. A reference case with simple geometry and three models with shed roofs are analyzed. Model 1 has orthogonal sheds on the roof; Models 2 and 3 have aerodynamic sheds on the roof. The methodology used is Computational Fluid Dynamic (CFD) simulation. It is shown that shed roof buildings can lead to very strong changes in the pressure distribution, because they introduce multiple areas of flow separation and recirculation across the facade. In addition, significant changes were identified with aerodynamic sheds in relation to orthogonal sheds.

1 Introduction

The building external pressure distribution assessment is essential for both evaluating wind loads and the performance of wind induced natural ventilation (CÓSTOLA; BLOCKEN; HENSEN, 2009; MONTAZERI, AZIZIAN, 2008; MONTAZERI et al., 2010; KARAVA; STATHOPOULOS; ATHIENTIS, 2004), usually expressed by the pressure coefficient (C_p) and with a natural influence in the thermal performance of a building. Thus, it is an important input data for several simulation programs of building thermal performance and airflow calculations, such as Energyplus, Aiolos, Contam and EDSL-TAS (WIT, 2001; ORME, 1999; CRAWLEY et al., 2008). The C_p is defined as the dimensionless quotient between the dynamic pressure measured at a point x on the facade of the building (P_x) and the dynamic pressure of the undisturbed airflow (P_d) (**Equation 1**) (AWBI, 1998; ETHERIDGE; SANDBERG, 1996). The undisturbed flow dynamic pressure (P_d) is the force per unit area exerted by the wind in an orthogonal plane to the direction of flow (**Equation 2**).

$$C_p = P_x / P_d \quad (1)$$

$$P_d = \rho V_{ref}^2 / 2 \quad (2)$$

Where:

P_d : dynamic fluid pressure (Pa)

V_{ref} : reference velocity measured at the same height as the building roof (m/s)

ρ : air specific mass (kg/m^3)

The pressure distribution on the walls of a building is influenced by a wide range of factors, including flow conditions of approach (STATHOPOULOS, 1997), urban environment (KIM; YOSHIDA; TAMURA, 2012), building geometry (UEMATSU; ISYUMOV, 1999) and wind direction (LEVITAN et al., 1991). In particular, a construction with complex geometry may affect the surface pressure distributions on the walls and roofs of buildings (STATHOPOULOS; ZHU, 1988). Naturally, C_p data available for designers about complex geometries is scarce due to the uniqueness of such cases. The existing data bases provide a limited number of C_p data for simplified building geometries, such as cubes, cylinders and parallelepipeds of different proportions, isolated or included into regular urban meshes (CÓSTOLA; BLOCKEN; HENSEN, 2009; ALLARD, 1998; SANTAMOURIS; WOUTERS, 2006; BITTENCOURT; CÂNDIDO, 2008; ORME; LIDDAMENT; WILSON, 1994; TOKYO POLITECHNIQUE UNIVERSITY, 2018; SANTOS, 2016). A common practice in the absence of these data is the use of C_p values obtained for other buildings of similar shapes which causes errors in the airflow analysis. In addition, the use of the mean C_p of the facade leads to significant errors in the airflow calculation, presenting differences of up to 40 % (CÓSTOLA et al., 2010).

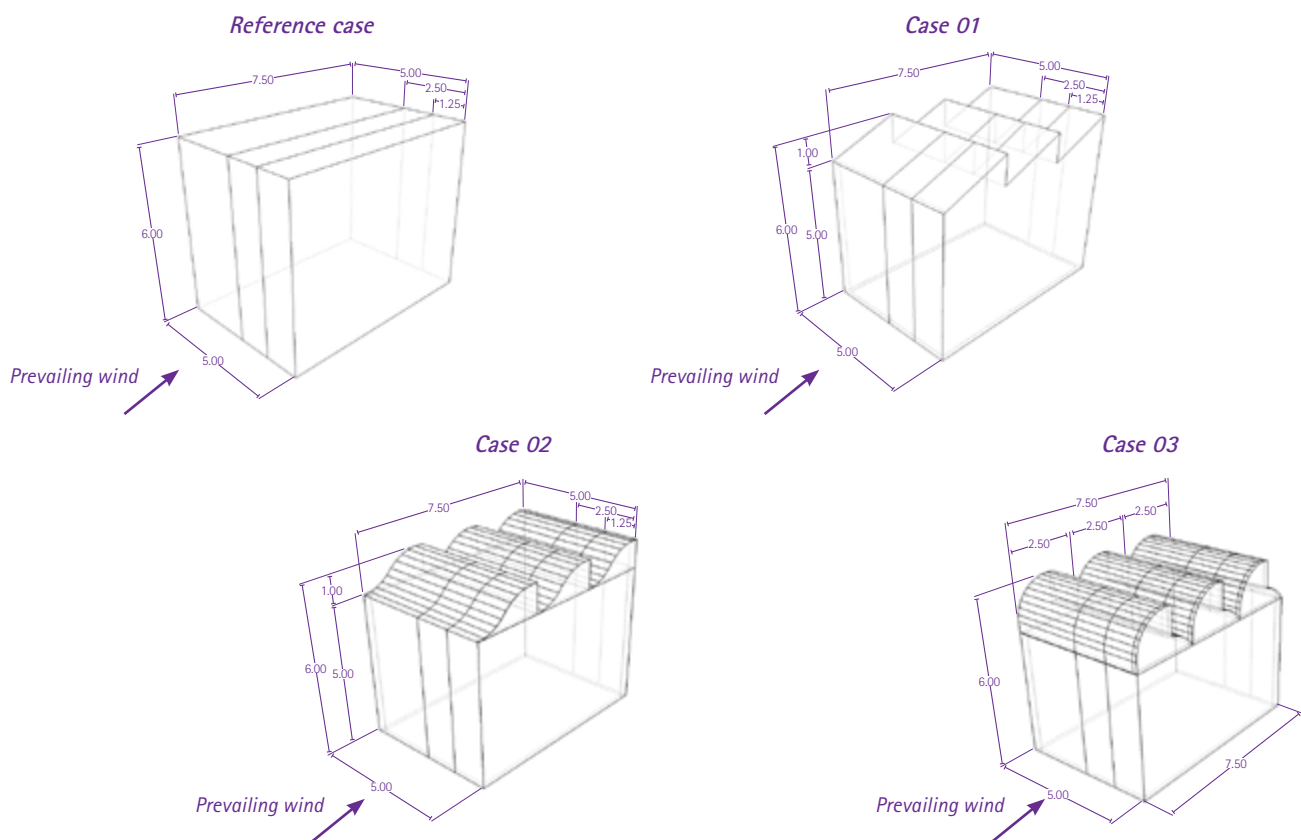
CFD simulations have been used on many occasions in the past to determine the wind-induced pressure distributions on the facades of buildings. Cóstola and Alucci (2011) state that the use of CFD to define C_p is feasible and constitutes an important alternative to wind tunnels. However, different simulation configurations lead to considerable deviations, both in absolute terms (up to ± 0.5 %) and in relative terms (up to 50 %). This work aims at evaluating the influence of roof shed geometry on the pressure coefficients of the surface of the closed buildings through CFD simulations.

2 Methodology

2.1 Description of the evaluated models

Four models with dimensions of 5 m x 7.5 m x 6 m (L x C x H) were evaluated: i) the reference case presents a simple geometry (parallelepiped); ii) case 1 has three sheds of orthogonal geometry (sawtooth) on the roof, with a slope of 22° and spaced from each other by 2.50 m; iii) case 2 sheds with a double curved aerodynamic geometry, and; iv) case 3 sheds with a simple curved aerodynamic geometry. The choice of shed geometries was based on the survey conducted by Lukiantchuki (2015) about the sheds designed by the architect Lelé in the Sarah Network hospitals. The chosen geometries referred to the Sarah hospitals of Salvador and Fortaleza, respectively. The evaluated models are totally closed (without openings). Cp values were evaluated on the building surface along vertical lines: the center line was located 2.50 m from the lateral wall. The edge line was located 1.25 m from the lateral wall (**Figure 1**). The sheds can work as air extractors or collectors depending on the opening orientation to the prevailing winds. This paper shows the data of the air-extractor shed situation. In a future work, these same data will be compared to a situation with air collector sheds.

Figure 1 – Evaluated models with centre and edge lines on the building surface (dimensions in meters)



Source: the authors

2.2 Computational Fluid Dynamic (CFD) simulation

The CFD simulations were performed using CFX 12.0 software. The three-dimensional models and computational domain were built using AutoCAD software. The rectangular domain dimensions followed the recommendations of Harries (2005), Franke et al. (2007) and Tominaga et al. (2008): windward and on the sides = 5H (25 m); height = 6H (30 m); and leeward = 15H (75 m). The height of the simulated model was 5 m (**Figure 2a**). The area of obstruction of the building in the domain is in accordance with the suggestion of Cost (2004), which recommends a value below 3 %. For all the simulations, a tetrahedral structured mesh was used whose global parameters were: (a) maximum element size 16; (b) natural size 4; and (c) cells in gap 8. The mesh was refined on the building surfaces, using a value of 0.10 m to improve the visualization of the airflow (**Figure 2b**). The combination of these parameters determines the number of mesh elements and the processing time of the simulations.

The domain conditions were: (a) inlet domain as Inlet and outlet domain as Outlet; (b) the domain sides and the domain ceiling as wall free slip, because it does not impose resistance to the parts of the domain where no important analyses are performed; and (c) the domain floor and building surfaces as wall no slip (with friction). For the computational simulations, the input velocity was $U = 2.5 \text{ m/s}$ ($Re = 9E5$), and the surroundings as a suburban environment with a value of $\alpha = 0.25$, adopted by Building Research Establishment (1978), using **Equation 3** as follows.

$$\frac{U}{U_{ref}} = \left(\frac{h}{h_{ref}} \right)^\alpha \quad (3)$$

Where:

U : average wind velocity at a certain point h (m/s);

U_{ref} : wind velocity measured at reference height (m/s);

h : building height to be evaluated for wind velocity (m);

h_{ref} : reference height of the wind velocity (10 m);

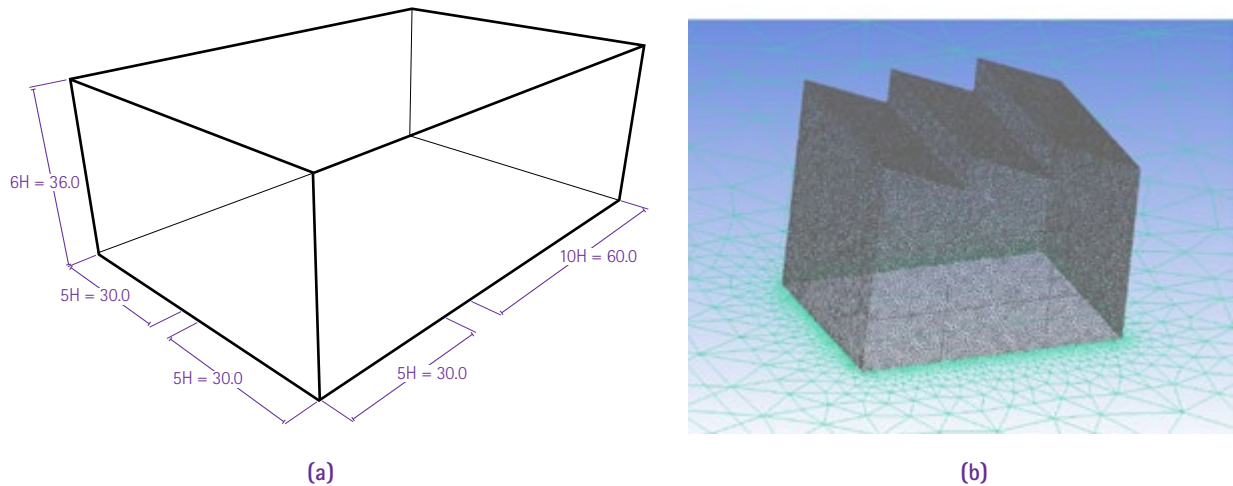
α : power law exponent of the atmospheric boundary layer (surrounding)

$Re = U \sqrt{A} / \nu$. Reynolds number

$A = L \times H$ (m^2).

ν : kinematic viscosity (m^2/s)

Figure 2 – (a) Dimensions of the computational domain and (b) tetrahedral mesh generated for all cases



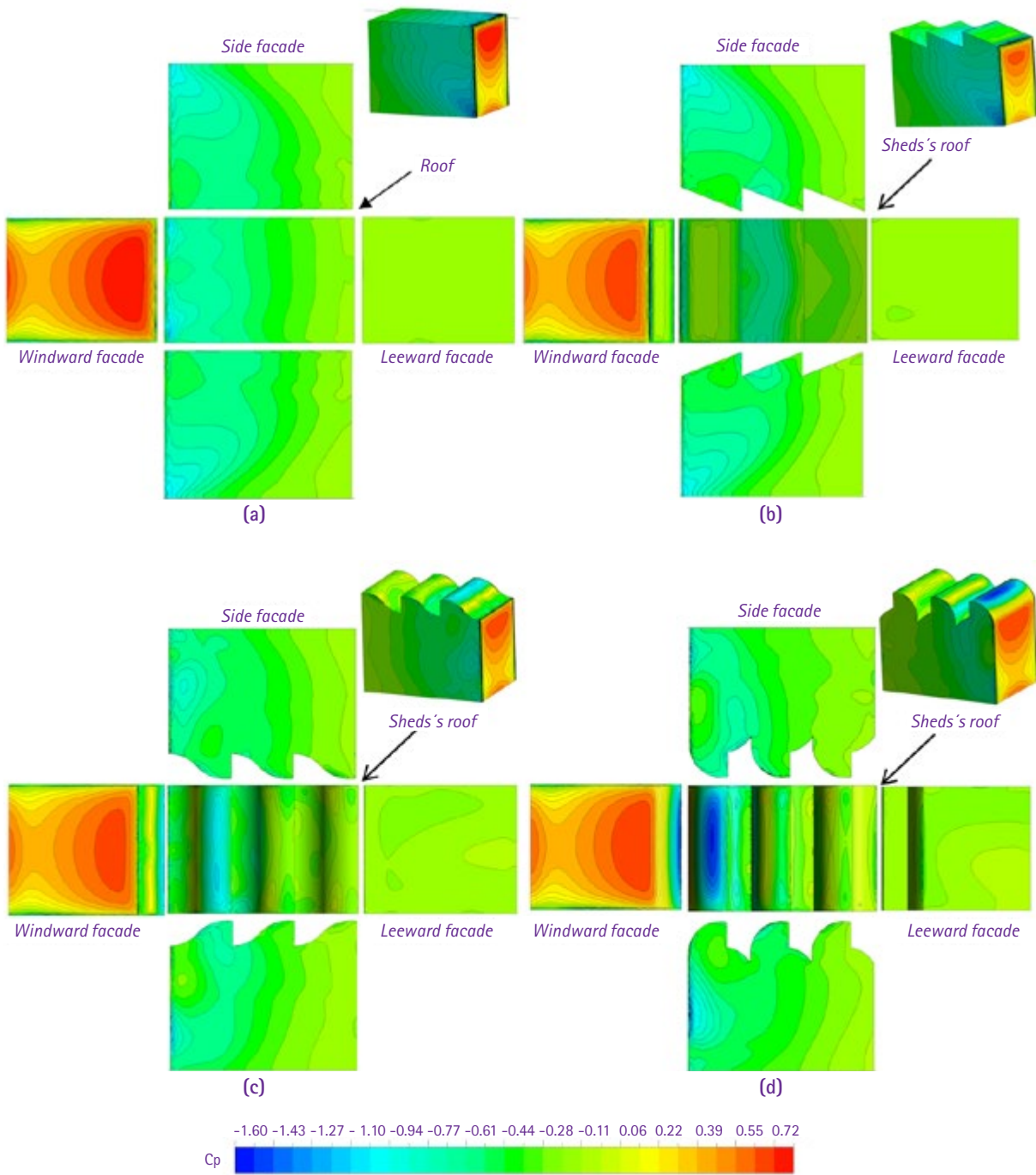
Source: the authors

A steady state condition was adopted for simulation, in an isothermal condition at $25\text{ }^{\circ}\text{C}$ (wind action). The turbulence model used was K-Epsilon which is common and well established in several studies of fluid dynamics and natural ventilation (CALAUTIT; HUGHES, 2014). The level of convergence was established when all residual levels reached a maximum value of 10^{-4} . The numbers of minimum and maximum iterations adopted were 600 and 6,000, respectively. These parameters were based on several studies using CFX software (BRANDÃO, 2009; CÓSTOLA, 2006; LEITE, 2008; PRATA, 2005).

3 Results

The impact of the buildings geometries on the C_p values of the surface of the models is investigated by comparing a simple geometry building (parallelepiped) with buildings of complex geometries which have different types of sheds on the roof. The analyzes were performed for the wind incidence perpendicular to the facade (0° - air extractor shed situation). **Figure 3** shows the C_p distribution on the surface of the four evaluated cases.

Figure 3 - C_p Distribution on the surfaces of the (a) reference case; (b) case 1; (c) case 2 e (d) case 3

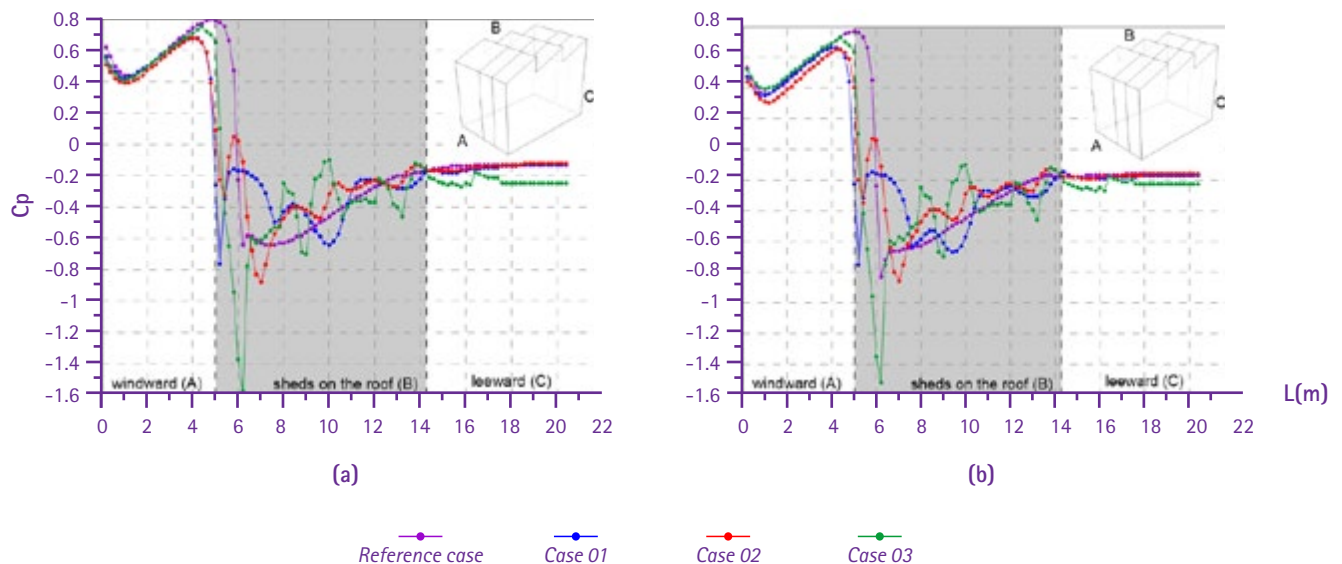


Source: the authors

The differences in the C_p distribution due to the addition of sheds in the coverage and the different geometries of these elements are evident. In the windward facade, the C_p distribution pattern on the surfaces is similar for all evaluated cases. However, there is a difference in values, especially in the mid-point of the facade, being higher for the reference case. The great divergence between the models is on the roof surface, both in the distribution pattern of pressures along the surface and as in the values, due to the presence of the sheds with different geometries.

In the lateral and leeward facades, differences were also recorded. The reference case and Model 1 have similar behavior, not presenting any significant change due to the change of the building's geometry. Models 3 and 4 show differences in the airflow distribution in these surfaces. The airflow affects perpendicularly on the windward face, contours the building at high velocities, causing shadows of wind on both sides of the building (separation of the flow) and, therefore, reduces the C_p values in these regions. As a result, it is noted that the smaller these values, the closer the windward face. As it approaches the leeward facade, the C_p becomes larger, that is, less negative tending to positive values. Due to the perpendicular incidence of the winds in the building, the C_p distribution on these surfaces is symmetrical (**Figure 3**). The analysis of the results is even more evident with **Figure 4** which compares the CFD simulation results of the C_p values along the vertical measurement axes (central and edge axes) for all analyzed cases.

Figure 4 - C_p distribution on the building surfaces in the (a) central axes and (b) edge axes

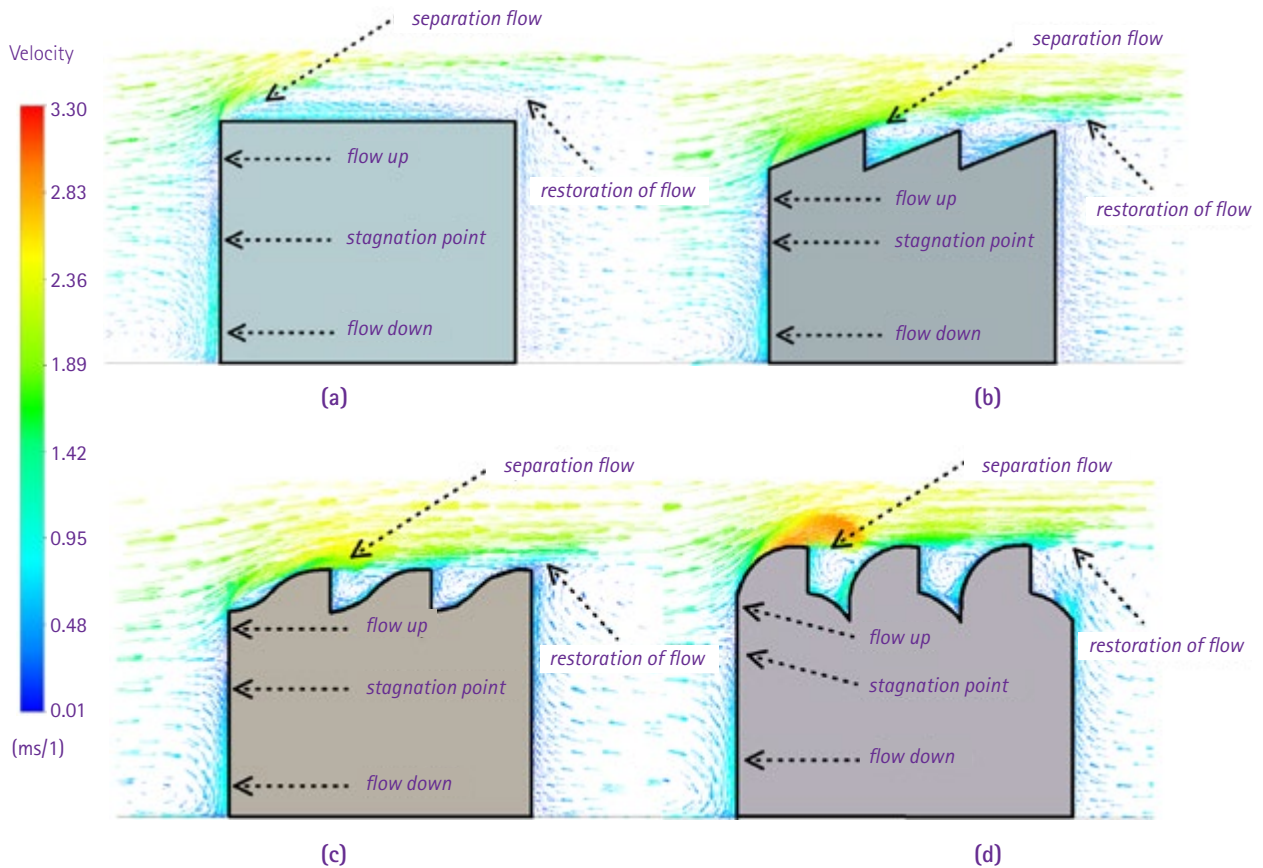


Source: the authors

Figure 4 confirms the complexity of the C_p distribution along the building with sheds on the roof and the impact of the building geometry on the C_p distribution on the building surface. In addition, an increase of this complexity is noticed when the sheds have aerodynamic geometries. At the windward facade, at half height of the facade, for the central and edge axis, the C_p values converge, presenting very similar data for the four cases which were analyzed. It is emphasized that, in simulations of thermal performance, the use of C_p values by the midpoint in the facade is common and, thus, this change in geometry would not lead to significant differences in these values. However, the use of an average value may lead to significant deviations in behaviour, especially in border areas. A significant difference is observed along the axis of the facade due to the different geometries, this difference being more expressive in case 3. The modification of the shed geometry produces a different profile of C_p along the facade, mainly in the upper region (near the sheds), recording lower pressure zones, when sheds are included in the building. This is because of the different curvatures in the separation between the facade and the roof. In case 3, most evident, the curvature of the shed keeps the flow adhering to the surface by accelerating it and, consequently, there is a reduction in pressure. The divergence registered which is significant in the performance of the internal airflow, was not captured by the average C_p of the facade, as previously recorded, indicating that the use of this value as input data of the thermal performance software creates false results.

In case 1, it is noted that this difference is due to the inclination of the sheds which allows the direct impact of the airflow on the roof and, later, a great wind shadow. In the reference case, its simple geometry forms a single wind shadow on the roof, originating from the airflow that faces the windward facade and generating C_p negative values along the entire roof surface. The region closest to the windward facade shows more negative values and, as it moves away from this region, the values are less negative. In case 1, the wind totally tangents the 1st shed with high velocities, presenting more negative C_p values. This slope of the shed generates a large zone of strongly depressive separation near the vertical surfaces, where the shed openings are usually located and, therefore, C_p values are more negative which favors the extraction of the air by the roof. This effect generates a wind shadow in the 2nd shed with air recirculation zones and lower C_p values. The same occurs in the 3rd shed, but with lower velocities and, thus, the C_p are larger (**Figures 4 and 5**).

Figure 5 - Velocity vectors on the surfaces of the (a) reference case, (b) case 1, (c) case 2 e (d) case 3



Source: the authors

Due to the aerodynamic geometry sheds in cases 2 and 3, the way that the airflow contours the geometries which reduces the frontal separation zone and significantly increases the velocity, causing a significant decrease in the C_p values. This is noticed at the highest point of the 1st shed: significantly higher velocities, with a more pronounced shadow zone and, consequently, more accentuated pressure drops in relation to the other cases, especially case 4 whose values are significantly lower (C_p around -0.95 and -1.60 for cases 3 and 4, respectively). In the latter sheds this effect continues to occur due to the airflow passing through the 2nd and 3rd sheds, being more intense in case 4 and non-existent in case 1. In the second part of the sheds of case 4, the higher C_p values due to the recirculations in this region at low velocities. It should also be noted that, in case 1, the pressure at the beginning of the roof shows an oscillation (Figure 4) due to the separation and re-collation areas formed between the edge and the shed.

4 Conclusions

Through this research, it is clear that the architectural design directly interferes with the C_p distribution on the building surfaces. The reference case, that is, the model with a simple parallelepiped geometry, is not representative of any of the typologies with analysed sheds, reinforcing that a change in the building geometry causes significant deviations in the C_p distribution on the building surfaces. This implies that accurate C_p values for these complex geometries are crucial for a successful evaluation of the performance of internal airflow. Using the C_p values available in the current databases for buildings that have elements in their geometries, which differ in simple geometries can lead to erroneous results that are incompatible with the reality. Thus, these standard values should not be used as input data for thermal performance simulation programs, but rather, the C_p values for each specific case must be evaluated.

5 References

- ALLARD, F. **Natural ventilation in buildings: a design handbook**. London: James x James, 1998.
- AWBI, H. B. **Ventilation of buildings**. London: E & FN Spon, 1998.
- BITTENCOURT, L.; CÂNDIDO, C. **Introdução à ventilação natural**. Maceió: Edufal, 2008.
- BRANDÃO, R. S. **As interações espaciais urbanas e o clima**. Tese (Doutorado em Arquitetura e Urbanismo) - Faculdade de Arquitetura e Urbanismo, Universidade de São Paulo, São Paulo, 2009.
- BUILDING RESEARCH ESTABLISHMENT. **Principles of natural ventilation**. Garston: BRE, 1978. (Digest, n. 210)
- CALAUTIT, J. K.; HUGHES, B. R. Wind tunnel and CFD study of the natural ventilation performance of a commercial multidirectional wind tower. **Building and Environment**, v. 80, p. 71-83, 2014.
- COST. **Cost Action 14: Recommendations on the use of CFD in predicting pedestrian wind environment**. Bruxelas: COST, 2004.
- CÓSTOLA, D. **Ventilação por ação do vento no edifício: procedimentos para quantificação**. 2006. Dissertação (Mestrado em Tecnologia da Construção) - Universidade de São Paulo, São Paulo, 2006.
- CÓSTOLA, D.; ALUCCI, M. P. Aplicação de CFD para o cálculo de coeficientes de pressão externos nas aberturas de um edifício. **Revista Ambiente Construído**, v. 11, n. 1, p. 145-158, jan./mar. 2011.

CÓSTOLA, D.; BLOCKEN, B.; HENSEN, J. L. M. Overview of pressure coefficient data in building energy simulation and airflow network programs. **Building Environment**, v. 44, n. 10, p. 2027-2036, Oct. 2009.

CÓSTOLA, D.; BLOCKEN, B.; OHBA, M.; HENSEN, J. L. M. Uncertainty in airflow rate calculations due to the use of surface-averaged pressure coefficients. **Energy and Buildings**, v. 42, p. 881-888, 2010.

CRAWLEY, D. B.; HAND, J. W.; KUMMERT, M.; GRIFFITH, B. T. Contrasting the capabilities of building energy performance simulation programas. **Building and Environment**, v. 43, n. 4, p. 661-673, 2008.

ETHERIDGE, D. W.; SANDBERG, M. **Building ventilation: theory & measure**. Chichester: John Wiles & Sons, 1996.

FRANKE, J.; HELLSTEN, A.; SCHLÜNZEN, H.; CARISSIMO, B. (Ed.). **Best practice guideline for the CFD simulation of flows in the urban environment**. Brussels: COST Office, 2007.

HARRIES, A. **Notas de aula**. São Paulo; CFX – FAU/USP, 2005.

KARAVA, P.; STATHOPOULOS, T.; ATHIENITIS, A. K. Wind driven flow through openings e a review of discharge coefficients. **International Journal of Ventilation**, v. 3, p. 255-66, 2004.

KIM, Y. C.; YOSHIDA, A.; TAMURA, Y. Characteristics of surface wind pressures on low-rise building located among large group of surrounding buildings. **Engineering Structures**, v. 35, p. 18-28, 2012.

LEITE, C. G. **Alterações da ventilação urbana frente ao processo de verticalização de avenidas litorâneas: o caso da avenida litorânea de São Luís/MA**. 2008. Dissertação (Mestrado em Arquitetura e Urbanismo) – Faculdade de Arquitetura e Urbanismo, Universidade de São Paulo, São Paulo, 2008.

LEVITAN, M. L.; MEHTA, K.; VANN, W. P.; HOLMES, J. D. Field measurements of pressures on the Texas tech building. **Journal of Wind Engineering and Industrial Aerodynamics**, v. 38, n. 2-3, p. 227-234, July/Aug. 1991.

LUKIANCHUKI, M. A. **Sheds extratores e captadores de ar para indução da ventilação natural em edificações**. 2015. Tese (Doutorado em Arquitetura e Urbanismo) – Instituto de Arquitetura e Urbanismo, Universidade de São Paulo, São Carlos, 2015.

MONTAZERI, H.; AZIZIAN, R. (2008). Experimental study on natural ventilation performance of one-sided wind catcher. **Building Environment**, v. 43, p. 2193-202, 2008.

MONTAZERI, H.; MONTAZERI, F.; AZIZIAN, R. MOSTAFAVI, S. Two-sided wind catcher performance evaluation using experimental, numerical and analytical modeling. **Renew Energy**, v. 35, p.1424-35, 2010.

ORME, M. L. **Applicable models for air infiltration and ventilation calculations**. [S.I.]: AIVC, 1999. 66 p. (Technical note 51).

ORME, M.; LIDDAMENT, M.; WILSON, A. **Numerical data for air infiltration and natural ventilation calculations**. [S.I.]: AIVC – Air Infiltration and ventilation Center, 1994. (Technical Note 44).

PRATA, A. R. **Impacto da altura de edifícios nas condições de ventilação natural no meio urbano**. 2005. Tese (Doutorado em Arquitetura e Urbanismo) – Faculdade de Arquitetura e Urbanismo, Universidade de São Paulo, São Paulo, 2005.

SANTAMOURIS, M.; WOUTERS, P. **Building ventilation: the state of the art**. London: Earthscan, 2006.

SANTOS, J. **Ação do vento em desfiladeiros urbanos**. 2016. Dissertação (Mestrado em Energia e Ambiente) – Universidade de Lisboa, Lisboa, 2016.

STATHOPOULOS, T. Computational wind engineering: past achievements and future challenges. **Journal of Wind Engineering and Industrial Aerodynamics**, v.67-68, p. 509-532, Apr./June, 1997.

STATHOPOULOS, T.; ZHU, X. Wind pressures on building with appurtenances. **Journal of Wind Engineering and Industrial Aerodynamics**, v. 31, n. 1-2, p. 265-281, Dec. 1988.

TOKYO POLYTECHNIQUE UNIVERSITY. School of Architecture and Wind Engineering. **TPU Aerodynamic Database**. Disponível em: <<http://wind.arch.t-kougei.ac.jp/system/eng/contents/code/tpu>>. Acesso em: 20 jun. 2018.

TOMINAGA, Y. et al. AIJ guidelines for practical applications of CFD to pedestrian wind environment around buildings. **Journal of Wind Engineering and Industrial Aerodynamics**, v. 96, n. 10-11, p. 1749-1761, Oct./Dec. 2008.

UEMATSU, Y.; ISYUMOV, N. Wind pressures acting on low-rise buildings. **Journal of Wind Engineering and Industrial Aerodynamics**, v. 82, n. 1-3, p. 1-25, 1999.

WIT, S. **Uncertainty in predictions of thermal comfort in buildings**. 2001. Thesis (PhD thesis) – School of Civil Engineering, University of Nottingham, Nottingham 2001.